# Cardiac bone marrow cell injection for chronic ischemic heart disease

Beeres, S.L.M.A.

# Chapter 11

Saskia L.M.A. Beeres[1]
Frank M. Bengel[2]
Jozef Bartunek[3]
Douwe E. Atsma[1]
Jonathan M. Hill[4]
Marc Vanderheyden[3]
Martin Penicka[5]
Martin J. Schalij[1]
William Wijns[3]
Jeroen J. Bax[1]

[1]Department of Cardiology, Leiden University Medical Center, Leiden, The Netherlands; [2]Division of Nuclear Medicine, Johns Hopkins University School of Medicine, Baltimore, Maryland, United States; [3]Cardiovascular Center Aalst, Aalst, Belgium; [4]Department of Cardiovacsular Diseases, King's College, London, United Kingdom; [5]CardioCenter, 3rd Medical School, Charles University and University Hospital, Prague, Czech Repulblic.

# Role of Imaging in Cardiac Stem Cell Therapy

*Journal of the American College of Cardiology 2007;49:1137-1148*

## Abstract

Stem cell therapy has emerged as a potential therapeutic option for cell death-related heart diseases. Pre-clinical and a number of early phase human studies suggested that cell therapy may augment perfusion and increase myocardial contractility. The rapid translation into clinical trials has left many issues unresolved, and emphasizes the need for specific techniques to visualize the mechanisms involved. Furthermore, the clinical efficacy of cell therapy remains to be proven. Imaging allows for in vivo tracking of cells and can provide a better understanding in the evaluation of the functional effects of cell-based therapies.

In this review, a summary of the most promising imaging techniques for cell tracking is provided. Among these are direct labeling of cells with super-paramagnetic agents, radionuclides, and the use of reporter genes for imaging of transplanted cells. In addition, a comprehensive summary is provided of the currently available studies investigating a cell therapy-related effect on left ventricular function, myocardial perfusion, scar tissue, and myocardial viability.

# Introduction

Stem cell transplantation is being widely investigated as a potential therapy for cell death-related heart diseases.[1] Several cell types, including embryonic stem cells,[2] skeletal myoblasts,[3,4] bone marrow-derived cells,[5-7] or cardiac resident stem cells[8,9] are being tested and pre-clinical studies have shown the potential of various approaches to repair acutely or chronically damaged myocardium.

In some experimental settings, transplantation of stem or progenitor cells after myocardial infarction reduces scar formation and fibrosis, and preserves cardiac function. Moreover, different subsets of progenitor cells were shown to augment perfusion. Both observations may be related to a direct physical effect (differentiation of progenitor cells to endothelial cells, smooth muscle cells and cardiomyocytes) and/or to the release of paracrine factors by progenitor cells, which prevent apoptosis of cardiomyocytes, modulate scar development or promote angiogenesis.[1]

On the basis of these encouraging pre-clinical studies, there is a growing number of early phase human studies that aim to demonstrate the feasibility and potential efficacy of cell-based therapies in the clinical setting.[10-35] This rapid translation into clinical studies has left a lot of questions concerning cell therapy unanswered. For example, the optimal cell type, the number of cells to be delivered, the most suitable route for cell delivery, and the optimal time point for cell delivery after myocardial infarction are unknown. Furthermore, the biodistribution of the therapeutic cells after delivery and the specific mechanism by which therapeutic cells contribute to functional improvement remain to be investigated. Imaging is crucial for in vivo tracking of cells and better understanding and evaluation of the effects of cell therapy. In this review, we have attempted to summarize the available evidence on imaging of cell therapy.



### Cell Tracking by Use of Non-invasive Imaging

The ideal imaging modality should provide integrated information related to the entire process of cell engraftment, survival and functional outcome. Clinically established parameters of non-invasive imaging, such as contractile function, perfusion, and viability of the myocardium, do not provide direct visualization of transplanted cells, their biology or function. Thus, a number of contrast agents and detectors for non-invasive, repeatable visualization of therapeutic cells in vivo have been pursued.[36] Such imaging approaches may not only refine the understanding of therapeutic mechanisms in pre-clinical studies but may also have direct clinical applications. Most of the available cellular molecular imaging techniques are also applicable in humans, and therefore may facilitate rapid translation of cell-based therapies into clinical practice. **Table 1** and **Figure 1** summarize labeling strategies for in vivo surveillance and tracking of various cell populations.

Radionuclide technology and magnetic resonance imaging (MRI) are best suited to meet such broad objective thanks to their resolution and clinical applicability, with MRI

**Table 1.** Techniques for in vivo imaging of labeled transplanted cells

| Method | Agent | Advantages | Disadvantages |
|---|---|---|---|
| MRI | SPIO | - High resolution<br>- No radiation | - Low sensitivity<br>- Signal may not reflect viable cells |
| Nuclear (direct labeling) | In-111 oxin<br>Tc-99m HMPAO<br>F18-FDG | - High sensitivity<br>- High translational capacity | - Radiation exposure to individual<br>- Potential effects of radiation on therapeutic cells<br>- Decay of radioactivity, signal may not reflect viable cells |
| Nuclear (reporter genes) | Various reporter genes / probes | - High biologic specificity (signal linked to viability)<br>- Studies of subcellular events (differentiation) | - Limited robustness of weak signal<br>- Concerns related to genetic modification |
| Optical | Luciferase / Luciferin<br>NIRF probes | - High sensitivity<br>- No radiation | - At present limited to small animals<br>- Not clinically applicable |

F18-FDG = fluorodeoxyglucose; HMPAO = exametazime; MRI = magnetic resonance imaging; NIRF = near infrared fluorescent; SPIO = super-paramagnetic iron oxide.



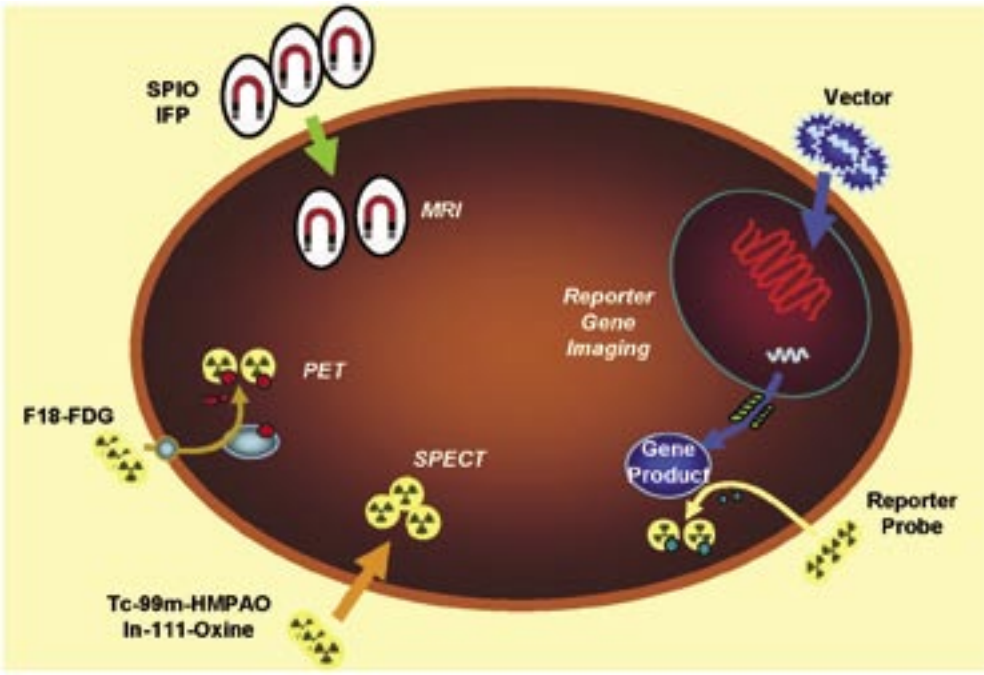


**Figure 1**
Approaches for cell tracking by non-invasive imaging. Cells are labeled directly for magnetic resonance imaging (MRI), positron emission tomography (PET), single-photon emission computed tomography (SPECT), or with a reporter gene for subsequent reporter-gene imaging using either of the techniques. F18-FDG=fluorodeoxyglucose; HMPAO=exametazime; IFP=iron fluorescent particle; SPIO=super-paramagnetic ironoxide.

**Table 2.** Nuclear imaging and MRI in cardiac stem cell therapy

| Process | MRI | Nuclear imaging |
|---|---|---|
| Cell homing / distribution | ++ | +++ |
| Cell survival | ? | +/- |
| Cell integration / differentiation | ? | Potential with reporter gene technology |
| Molecular effects | + | + |
| Structural tissue and organ remodeling | ++ | - |
| LV regional and global function | +++ | +/- |
| Perfusion / metabolism | ++ | +++ |

LV = left ventricular; MRI = magnetic resonance imaging.



having some advantages in terms of spatial resolution (**Table 2**). Cells can be labeled directly with super-paramagnetic iron oxide agents or radionuclides before their application for subsequent in vivo visualization of their distribution. Additionally, genetic labeling with reporter genes that can be traced with imaging probes has been introduced, which will allow for repeatable tracking of cellular and subcellular function over a longer period of time. The use of non-invasive imaging modalities in pre-clinical cell therapy studies revealed key aspects of cell biology that will not be observed by other approaches except for histological analysis. In particular, the ability to dynamically follow cell trafficking and survival over longer periods of time contributed to the understanding of the potential mechanism of benefit.

### Direct Labeling of Cells using Magnetic Resonance Agents

MRI has become a key surrogate endpoint to demonstrate efficacy in early phase, small sized studies.[37] MRI can provide detailed morphological and functional information and therefore seems ideally suited to integrate efficacy assessments with the capability for cell tracking. The potential for assessing engraftment of therapeutic cells was quickly realized and investigations are now focusing on refining contrast agents to ensure maximum signal for minimum labeling. Initial animal model studies using micron scale particles[38,39] or nanoparticles of iron oxide[40,41] showed the potential for non-toxic labeling of hematopoietic bone marrow-derived and mesenchymal stem cell populations without affecting their transdifferentiation capacity. In the cardiovascular setting, this cell labeling technology was coupled with direct delivery methods using endomyocardial injections, demonstrating that transplanted cells could be imaged shortly after delivery with a high degree of spatial resolution using MRI (**Figure 2**).[40] Iron oxide labeling can also be used to track smaller numbers of cells in homing experiments allowing for in vivo identification of mesenchymal stem cells that migrated to infarcted myocardium after intravenous administration.[41] Yet, in the described studies in the preceding text, the lowest detectable number of cells was $10^5$ with the use of conventional MRI scanners without any sequence modification. This threshold of detection can be lowered using high field magnets (11.7

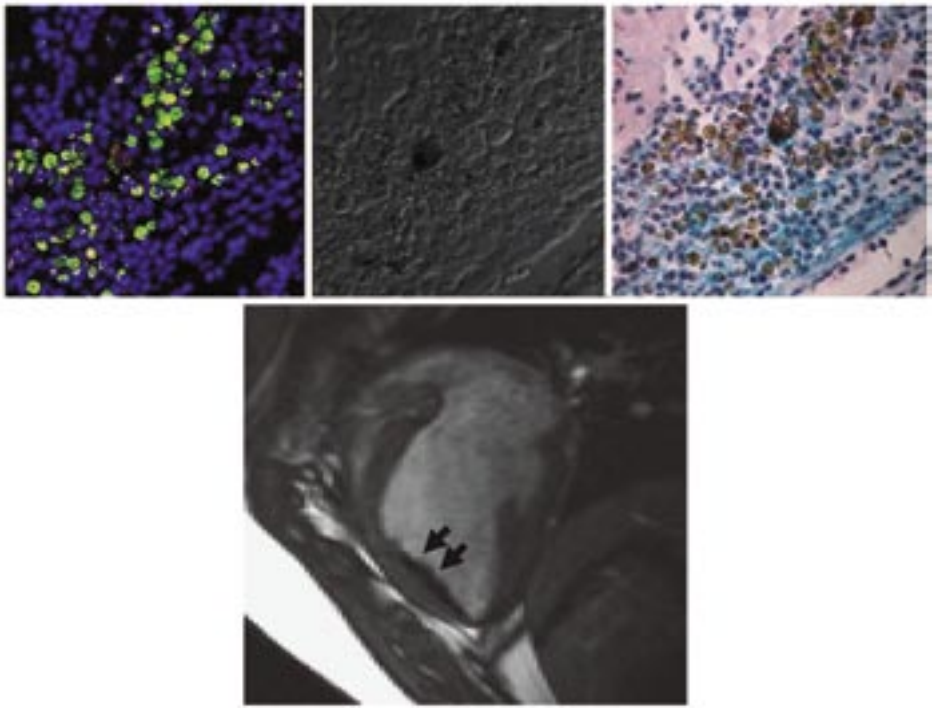

**Figure 2**
Magnetic resonance imaging (MRI) labeling using combined modality imaging agent. Fluorescent green component of iron-fluorophore-labeled porcine mesenchymal stem cells delivered by intramyocardial injection with nuclei stained blue (left). Same panel imaged using Nomarski optics (middle). Haemotoxylin/eosin stain of same panel with iron-labeled cells appearing brown (right).
MRI long-axis slice of a porcine left ventricle after anteroapical intramyocardial injection of iron-fluorophore-labeled mesenchymal stem cells (bottom). The black area on the endomyocardial border (arrows) is the signal void created by the iron-labeled cells

Tesla) such that single cells containing a single iron particle can be detected and tracked.[42] There are potential theoretical disadvantages to the use of magnetic labeling. Most importantly, the imaging signal is not directly linked with cell viability. There is a risk for release of iron oxide after cell death and its accumulation in bystander cells confounding any quantitative assessment of cell trafficking. In addition, cell division can dilute the magnetic label within only a few cell divisions. Novel direct labeling techniques like Clio-tat peptides[43] or magnetic relaxation switches[44] are under development in pre-clinical studies and could help overcome some of these limitations in the future. Despite minimal effect of iron oxide particles on in vitro proliferative capacity and cell viability,[38] there are recent data raising concern about the impact on the differentiation capacity of mesenchymal stem cells along a chondrogenic differentiation pathway.[45] On the other hand, this effect may be compound specific, because the two Food and Drug Administration-approved iron oxide based agents affect neither haematopoietic nor mesenchymal stem cell function or differentiation capacity.[46] Before clinical application, future work is required to investigate the effect of iron-labeling on stem cell proliferation and differentiation.

**Direct Labeling of Cells using Radionuclides**

Direct labeling of cells with radionuclides provides the advantage of a lower background signal as compared to MRI. However, higher sensitivity is achieved at the cost of lower spatial resolution. Various clinically applicable radionuclides have been used, based on previously established protocols for leukocyte or thrombocyte scintigraphy. Direct labeling with radionuclides appears highly informative for clinical studies addressing homing and biodistribution after cell injection. In-111-labeled endothelial and hematopoietic progenitor cells were found to accumulate in infarcted rat myocardium after intraventricular injection (**Figure 3**), but the overall radioactivity in the heart was only around 4.7% of the injected dose.[47] These data suggest that only a small number of cells ultimately home to injured myocardium, but they also corroborate the high sensitivity of the nuclear imaging technique. In another study using In-111-labeled mesenchymal stem cells in pigs, accumulation in the lungs was observed early after intravenous injection, which was found to obscure assessment of myocardial cell trafficking.[48] This observation was confirmed in rats by another group, using Tc-99m exametazime (HMPAO) for labeling of bone marrow-derived mesenchymal stem cells and observing entrapment of the donor cells in the lungs.[49] More recently, homing of In-111-labeled mesenchymal stem cells to infarcted myocardium was successfully visualized in a dog model using single-photon emission computed tomography (SPECT)-CT.[41] Finally, the positron emission

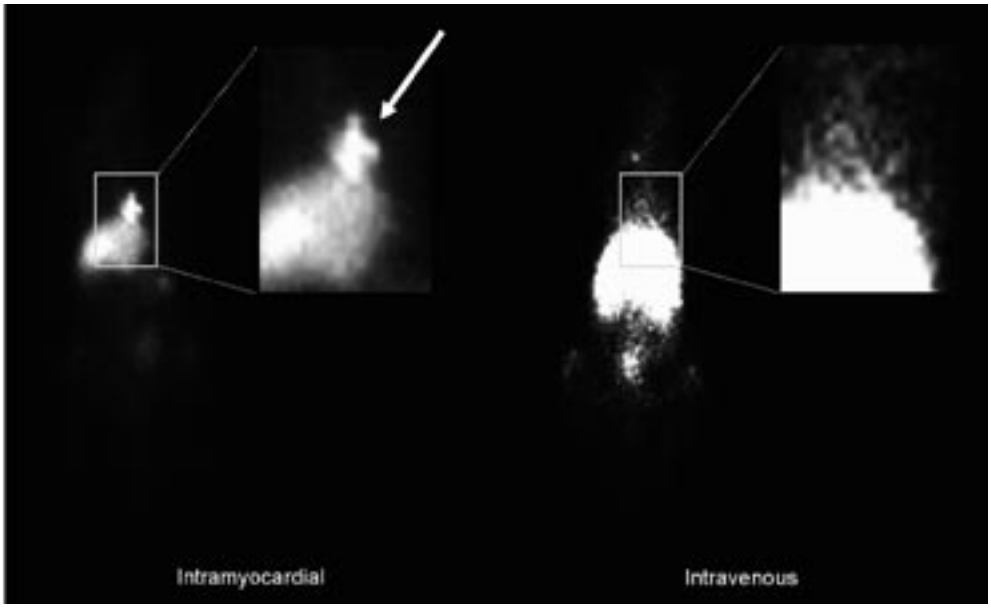


**Figure 3**

Tracking of In-111-labeled endothelial progenitor cells in the rat heart. After experimental myocardial infarction, $10^6$ In-111-labeled cells were injected intramyocardially (left) or intravenously (right). Shown are planar scintigraphic images of the whole animal, along with magnification of the cardiac area. Significant cardiac retention of cells in the heart is only identified after intramyocardial injection (arrow).

tomography (PET) tracer F18-fluorodeoxyglucose (F18-FDG) has been used for labeling and imaging of bone-marrow cells in humans. Myocardial accumulation of cells was demonstrated after intracoronary infusion, but not after intravenous delivery. With immunomagnetically-enriched CD34-positive cells, 14-39% of total injected radioactivity was detected in infarcted myocardium after intracoronary injections, preferentially in the border zone.[50] Other data indicate that radiolabeling could be used to assess early kinetics after cell injection. Tc-99m-HMPAO-labeling of mononuclear cells indicated that cardiac engraftment of cells is a dynamic process: the radioactivity uptake by the heart was 5% at 2 hours and 1% at 18 hours after transcoronary cell transplantation in a patient with acute myocardial infarction.[51] These data support the translational potential of nuclear imaging to guide cell therapy approaches from pre-clinical to clinical applications and to provide mechanistic information in applications like intracoronary administration with higher sensitivity than MRI. Future work should aim to prolong the half-life time of radioisotopes in order to prevent loss of the imaging signal within a few days.



**Reporter Genes for Cardiovascular Cell Imaging**

The usefulness of reporter genes for imaging of gene transfer to the myocardium has been established recently.[52] This principle may be expanded to imaging of cell-based therapies. A reporter gene of choice can be transferred to cells for genetic labeling, prior to their in vivo administration. After application, cells can then be detected by an intravenously administered, radio-labeled or optical reporter probe which is specific for the reporter gene and which accumulates solely in the transduced therapeutic cells (**Figure 4**). Because accumulation of the reporter probe requires expression of the reporter gene and activity of the reporter gene product, the imaging signal will be dependent on viability of the therapeutic cells. This is in contrast to direct "passive" labeling techniques and provides a more specific readout. Additionally, imaging can be performed repeatedly and is not limited by radioactive decay of the initial label load. Observation of genetically-labeled cells is thus possible over a long period of time, and may only be limited by epigenetic silencing.[53]

Proof of principle for imaging of genetically-labeled cells was obtained using rat cardiomyoblasts, which were infected ex vivo with adenovirus carrying the HSV1-sr39tk and luciferase reporter genes. Cell-specific in vivo optical and micro PET imaging was feasible for up to 2 weeks following direct injection of cells into the myocardium of nude rats. For optical imaging, $5x10^5$ cells were detectable, while PET images were obtained using $3x10^6$ cells.[54] Subsequent pre-clinical studies used reporter gene labeling to demonstrate usefulness of novel intramyocardial injection techniques and assess cell survival, proliferation and migration over a longer period of time.[55,56]

Importantly, genetic labeling also holds promise to provide insights into sub-cellular mechanisms that take place within therapeutic cells. Reporter genes may be expressed under control of restrictive promoters which are sensitive to certain endogenous molecules. Despite bearing a conceptual promise, the use of reporter gene imaging to

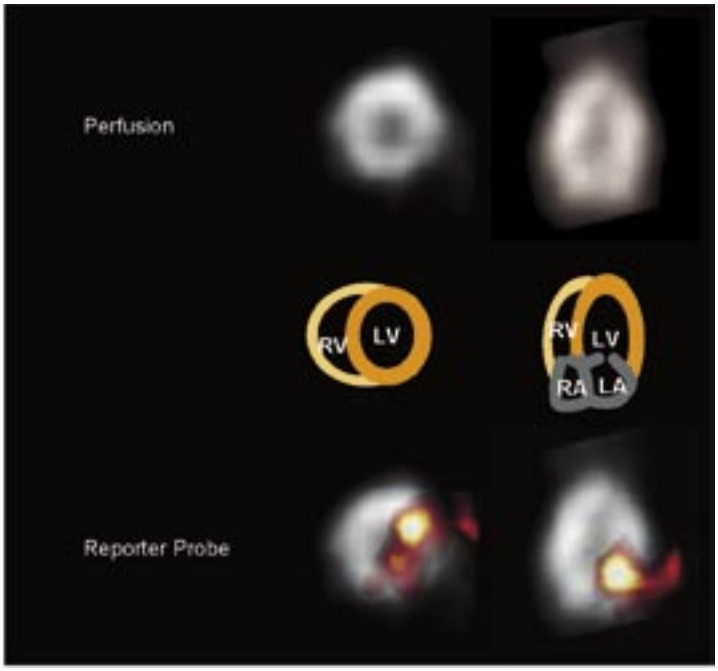


**Figure 4**
Tracking of genetically-labeled progenitor cells by positron emission tomography. A total of $3x10^6$ endothelial progenitor cells transfected with the sodiumiodide symporter gene were injected intramyocardially in a healthy rat. After injection of N-13 ammonia, homogeneous myocardial perfusion is shown in grayscale on the top. Perfusion images are overlayed with images of reporter gene expression (bottom), obtained after injection of I-124 sodiumiodide (red/yellow). Regional accumulation of the reporter probe depicts presence of viable transplanted cells at the injection site in the lateral wall. LA=left atrium; LV=left ventricle; RA=right atrium; RV=right ventricle.

monitor cell transplantation is still limited to animal model studies. In order to proceed from bench to bedside, further work is required to develop non-immunogenic probes, improve transfection stability and reduce the interference of transfection with the cell function and desired molecular effect. Strength of the imaging signal is critical and additional work is necessary to establish a robust approach for cell visualization which is also practical for use in the clinical setting.

### Imaging To Evalute Functional Effects Of Cell Therapy

Imaging may be particularly helpful in evaluating the functional effects of cell therapy. The various clinical studies have mainly focused on detection of differences in left ventricular (LV) function, myocardial perfusion, infarct size, and myocardial viability.

### Left Ventricular Function

**Table 3** summarizes the 17 available studies (including 10 or more patients) that have evaluated changes in LV function after cell therapy. In total, 526 patients underwent cell

**Table 3.** Effect of cell therapy on left ventricular function and volumes

| | No. of Patients | Setting / Study design | Route of delivery | Cell Type |
|---|---|---|---|---|
| Strauer et al. [10] | 10 vs. 10 controls | AMI / Observational, Control + | Intracoronary | $2.8x10^7$ BMC |
| TOPCARE-AMI [11-13] | 29 BMC 30 CPC | AMI / Observational, Control - | Intracoronary | $2.1x10^8$ BMC $1.6x10^7$ CPC |
| BOOST [16;17] | 30 vs. 30 controls | AMI / Randomized, Sham - | Intracoronary | $2.4x10^9$ BMC |
| Fernández-Avilés et al. [18] | 20 vs. 13 controls | AMI / Observational, Control + | Intracoronary | $7.8x10^7$ BMC |
| Chen et al.[19] | 34 vs. 35 controls | AMI / Randomized, Sham + | Intracoronary | $4.8\text{-}6.0x10^{10}$ BMC |
| Bartunek et al. [20] | 19 vs. 16 controls | AMI / Observational, Control + | Intracoronary | $1.3x10^7$ BMC |
| Janssens et al. [21] | 33 vs. 34 controls | AMI / Randomized, Sham + | Intracoronary | $4.8x10^8$ BMC |
| REPAIR-AMI [22] | 101 vs. 103 controls | AMI / Randomized, Sham + | Intracoronary | $2.4x10^8$ BMC |
| ASTAMI [23] | 50 vs. 50 controls | AMI / Randomized, Sham - | Intracoronary | $6.8x10^7$ BMC |
| TOPCARE-CHD [24] | 28 BMC vs. 24 CPC vs. 23 controls | CMI / Randomized, Sham - | Intracoronary | $2.1x10^8$ BMC $2.2x10^7$ CPC |
| IACT [25] | 18 vs. 18 controls | CMI / Observational, Control + | Intracoronary | $9x10^7$ BMC |
| Katritsis et al. (26) | 11 vs. 11 controls | CMI / Observational, Control + | Intracoronary | $2\text{-}4x10^6$ BMC and EPC |
| Fuchs et al. [27;28] | 27 | AP / Observational, Control - | Intramyocardial | $7.8x10^7$ BMC |
| Beeres et al. [29-31] | 25 | AP / Observational, Control - | Intramyocardial | $8.4x10^7$ BMC |
| Perin et al. [32;33] | 14 vs. 7 controls | HF / Observational, Control + | Intramyocardial | $3x10^7$ BMC |
| Erbs et al. [34] | 13 vs. 13 controls | CTO / Randomized, Sham + | Intracoronary | $6.9x10^7$ G-CSF-mobilized cells |
| MAGIC [35] | 10 vs. 17 controls | AMI/CMI / Randomized, Sham - | Intracoronary | $1.5x10^9$ G-CSF-mobilized cells |

AMI = acute myocardial infarction; AP = angina pectoris; BMC = bone marrow cells; CMI = chronic myocardial infarction; CPC = circulating progenitor cell; CTO = chronic total occlusion; EPC = endothelial progenitor cell; G-CSF = granulocyte-colony stimulating factor; HF = heart failure; LV = left ventricular; LVEDV = left ventricular

| | Follow-up (Months) | LVEF | LVESV | LVEDV | Regional Contractility | Technique Used |
|---|---|---|---|---|---|---|
| | 3 | = | ↓ | = | ↑ wall motion in infarct zone | LV angiography<br>RNV |
| | 12 | ↑ ( 9.3%) | ↓ | = | ↑ wall motion in infarct zone | LV angiography<br>Cine MRI |
| | 18 | = | = | = | = | Cine MRI |
| | 6 | ↑ ( 5.8%) | ↓ | = | ↑ wall motion in infarct zone | Cine MRI |
| | 6 | ↑ (18.0%) | ↓ | ↓ | ↑ wall motion in infarct zone | LV angiography |
| | 4 | ↑ ( 7.0%) | ↓ | = | ↑ wall motion | LV angiography |
| | 4 | = | = | = | = | Cine MRI |
| | 4 | ↑ (5.5%) | = | = | ↑ wall motion in infarct zone | LV angiography |
| | 6 | = | = | = | NA | Gated SPECT<br>Cine MRI |
| | 3 | ↑ (2.9%) | = | = | ↑ wall motion in infarct zone | LV angiography |
| | 3 | ↑ ( 8.0%) | NA | NA | ↑ wall motion in infarct zone | LV angiography |
| | 4 | = | = | = | ↑ wall motion | 2D echo<br>RNV |
| | 3 | = | NA | NA | = | 2D echo |
| | 12 | ↑ ( 4.0%) | ↓ | = | ↑ wall motion | Gated SPECT<br>Cine MRI |
| | 12 | = | ↓ | NA | NA | LV angiography<br>2D echo |
| | 3 | ↑ ( 7.2%) | = | = | ↑ wall motion | Cine MRI<br>Gated SPECT |
| | 6 | ↑ ( 6.4%) | ↓ | NA | NA | Gated SPECT<br>2D echo |

end-diastolic volume; LVEF = left ventricular ejection fraction; LVESV = left ventricular end-systolic volume; MRI = magnetic resonance imaging; NA = not available; RNV = radionuclid ventriculography; Sham = placebo-controlled; SPECT = single photon emission computed tomography.

therapy in these studies. Ten studies were performed in the setting of acute myocardial infarction, and 7 studies were performed in the setting of chronic ischemic heart disease. Assessment of function was performed ranging from 3 to 18 months after cell therapy.

Ten studies showed an improvement in left ventricular ejection fraction (LVEF), indicating improved systolic function. The majority of studies indicated small improvements in LVEF (range 2.9 to 9.3%), but Chen et al. demonstrated in 34 patients with acute myocardial infarction an improvement of 18%.[19] Different techniques were used to assess LV function and volumes, including LV angiography, 2D echocardiography, gated SPECT, radionuclid ventriculography and MRI. The most accurate assessment of LVEF and LV volumes is MRI, and Fernández-Avilés and colleagues demonstrated an increase of 5.8% in LVEF as assessed by MRI, whereas no improvement was seen in control patients.[18] The global improvement in LVEF was mainly related an improvement of regional LV function in the infarct zone, although improvement of function in the infarction border zone has also been reported.



Left ventricular end-diastolic volume (LVEDV) remained unchanged in most (12/17) studies, indicating absence of LV reverse remodeling. However, since LVEDV did not increase either, one could argue that cell therapy prevented progressive LV dilatation. In support of this, Bartunek et al. demonstrated that the LVEDV index remained unchanged in patients undergoing cell therapy, whereas an increase from 91±7 ml/m$^2$ to 103±9 ml/m$^2$ ($P<0.05$) was observed in control patients.[20]

The improvement of LVEF may be a time-dependent process; in the BOOST trial sequential measurements were performed in 30 bone marrow cell transfer patients and in 30 control patients, at 6 and 18 months. At 6 months, MRI demonstrated an increase in LVEF of 6.7% in bone marrow cell transfer patients, as compared to 0.7% in controls ($P<0.01$). However, at 18 months the LVEF change was not significantly different between the 2 groups (+5.9% vs. +3.1%; P=NS). Analysis of the time course of LVEF improvement however, revealed a significantly faster recovery of LVEF in the bone marrow cell transfer patients than in control patients ($P<0.01$).[17]

**Myocardial Perfusion**

A total of 11 studies (including 239 patients) evaluated the effect of cell therapy on perfusion (**Table 4**). Five studies were performed in the setting of acute myocardial infarction, 3 studies in patients with chronic infarction and 3 studies in patients with stress-induced ischemia. Assessment of perfusion was performed ranging from 3-12 months after therapy. The clinically available tools for assessment of myocardial perfusion include nuclear imaging with PET or SPECT, MRI using first-pass perfusion, or myocardial contrast echocardiography. In addition, coronary blood flow can invasively be assessed using the Doppler flow wire at rest and during pharmacological stress. Subsequent calculation of the coronary flow reserve provides insight in the integrity of both the epicardial conduit arteries and the distal microvascular bed.

In 9 of 11 currently available studies SPECT was used, and only Janssens et al. used PET to

**Table 4** Effect of cell therapy on myocardial perfusion

| | No. of Patients | Setting / Study design | Route of Delivery | Cell Type | Follow-up (Months) | Main Findings | Technique Used |
|---|---|---|---|---|---|---|---|
| Strauer et al. [10] | 10 vs. 10 controls | AMI / Observational, Control + | Intracoronary | 2.8x10$^7$ BMC | 3 | ↓ Perfusion defect | Tl-201 SPECT (rest) |
| TOPCARE-AMI[11-15] | 29 BMC 30 CPC | AMI / Observational, Control - | Intracoronary | 2.1x10$^8$ BMC 1.6x10$^7$ CPC | 4 | ↓ Perfusion defect ↑ Coronary flow reserve | Tl-201 SPECT (rest) Intracoronary Doppler |
| Bartunek et al. [20] | 19 vs. 16 controls | AMI / Observational, Control + | Intracoronary | 1.3x10$^7$ BMC | 4 | ↓ Perfusion defect | Tc-99m sestamibi SPECT (rest) |
| Janssens et al. [21] | 33 vs. 34 controls | AMI / Randomized, Sham + | Intracornary | 4.8x10$^8$ BMC | 4 | = Perfusion defect | C-11 acetate PET (rest) |
| IACT [25] | 18 vs. 18 controls | CMI / Observational, Control + | Intracoronary | 9x10$^7$ BMC | 3 | ↓ Perfusion defect | Tc-99m tetrofosmin SPECT (rest) |
| Katritsis et al. [26] | 11 vs. 11 controls | CMI / Observational, Control + | Intracoronary | 2-4x10$^6$ BMC and EPC | 4 | ↓ Perfusion defect | Tc-99m sestamibi SPECT (stress-rest) |
| Fuchs et al. [27;28] | 27 | AP / Observational, Control - | Intramyocardial | 7.8x10$^7$ BMC | 3 | ↑ Stress perfusion in injected territories = Stress perfusion in remote territories | Tl-201 SPECT (rest) Tc-99m sestamibi SPECT (stress) |
| Beeres et al. [29-31] | 25 | AP / Observational, Control - | Intramyocardial | 8.4x10$^7$ BMC | 12 | ↓ Extent of ischemia | Tc-99m tetrofosmin SPECT (stress-rest) |
| Perin et al.[32;33] | 14 vs. 7 controls | HF / Observational, Control + | Intra-myocardial | 3x10$^7$ BMC | 12 | = Perfusion defect ↓ Extent of ischemia | Tc-99m sestamibi SPECT (stress-rest) |
| Erbs et al. [34] | 13 vs. 13 controls | CTO / Randomized, Sham + | Intracoronary | 6.9x10$^7$ G-CSF- mobilized cells | 3 | ↑ Coronary flow reserve | Intracoronary Doppler |
| MAGIC [35] | 10 vs. 17 controls | AMI/ CMI / Randomized, Sham - | Intracoronary | 1.5x10$^9$ G-CSF- mobilized cells | 6 | ↓ Perfusion defect = Coronary flow reserve | Tl-201 SPECT (rest) Tc-99m sestamibi SPECT (stress) Intracoronary Doppler |

AMI = acute myocardial infarction; AP = angina pectoris; BMC = bone marrow cells; CMI = chronic myocardial infarction; CPC = circulating progenitor cell; CTO = chronic total occlusion; EPC = endothelial progenitor cell; HF = heart failure; G-CSF = granulocyte-colony stimulating factor; PET = positron emission tomography; Sham = placebo-controlled; SPECT = single photon emission computed tomography.

evaluate the effect of cell therapy on perfusion.[21] It should be emphasized however that only PET permits absolute quantification of myocardial perfusion, whereas SPECT provides information on relative changes in tracer uptake.

The majority (10 of 11) studies demonstrated some effect of cell therapy on perfusion. For example, Bartunek et al., using resting Tc-99m sestamibi SPECT, demonstrated a decrease in resting perfusion defect size at 4 months. Conversely, defect size did not change in control patients.[20] Similar results were reported by other groups. Of note, the only study with PET could not demonstrate an increase in perfusion.[21]

The majority of the studies evaluated only resting perfusion, but few studies evaluated both rest and stress perfusion with SPECT. Beeres et al. demonstrated in patients with refractory angina a significant decrease in the number of segments with stress-inducible ischemia.[31] A patient example with a reduction in ischemia is shown in **Figure 5**. Perin et al. presented similar results with stress-rest Tc-99m sestamibi SPECT in heart failure patients.[33]



Three studies used intracoronary Doppler with 2 of 3 studies showing an improvement in coronary flow reserve. For example, a substudy of the TOPCARE-AMI trial revealed that progenitor cell therapy was associated with complete restoration of coronary flow reserve due to a substantial improvement of maximal coronary vascular conductance capacity.[15]

**Infarct Size**

In the clinical setting, 12 studies (including 355 patients) evaluated the effect of cell therapy on infarct size (**Table 5**). Seven studies were performed in the setting of acute infarction, whereas 5 were performed in patients with chronic infarction. Assessment of scar tissue was performed ranging from 3 to 18 months after therapy. A variety of techniques is available to assess infarct size, including techniques that directly visualize

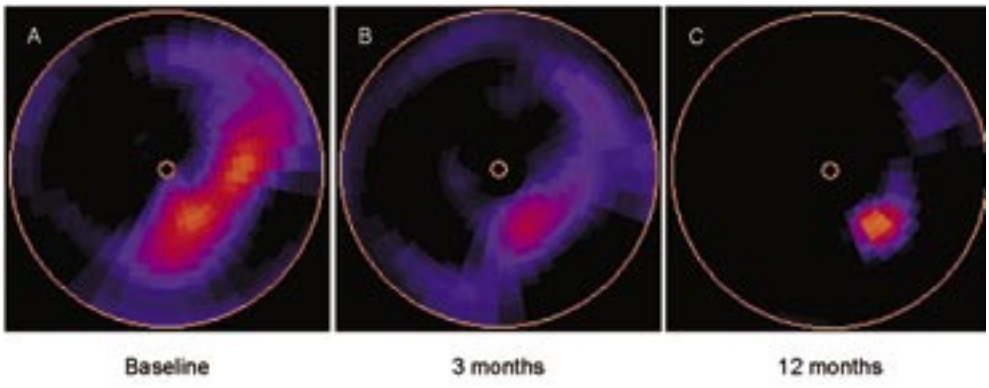


**Figure 5**

Tc-99m tetrofosmin single-photon emission computed tomography polar maps of a patient with stress-induced ischemia in the inferolateral myocardium at baseline (left). Three months after intramyocardial injection of autologous bone marrow-derived mononuclear cells there is a reduction in the extent of stress-induced ischemia (middle). The effect is sustained at 12 months follow-up (right). Reprinted from reference #31, with permission.

**Table 5** Effect of cell therapy on infarct size

| | No. of Patients | Setting / Study design | Route of Delivery | Cell Type | Follow-up (Months) | Main Findings | Technique Used |
|---|---|---|---|---|---|---|---|
| Strauer et al. [10] | 10 vs. 10 controls | AMI / Observational, Control + | Intracoronary | $2.8x10^7$ BMC | 3 | ↓ Infarct size (% of dysfunctional segments) | LV angiography |
| TOPCARE-AMI [11-14] | 29 BMC<br>30 CPC | AMI / Observational, Control - | Intracoronary | $2.1x10^8$ BMC<br>$1.6x10^7$ CPC | 12 | ↓ Infarct size (contrast-enhanced volume) | Contrast-enhanced MRI |
| BOOST [16;17] | 30 vs. 30 controls | AMI / Randomized, Sham - | Intracoronary | $2.4x10^9$ BMC | 18 | = Infarct size (contrast-enhanced volume) | Contrast-enhanced MRI |
| Fernández-Avilés et al. [18] | 20 vs. 13 controls | AMI / Observational, Control + | Intracoronary | $7.8x10^7$ BMC | 6 | ↓ Infarct size (number of dysfunctional segments) | Cine MRI |
| Chen et al. [19] | 34 vs. 35 controls | AMI / Randomized, Sham + | Intracoronary | $4.8\text{-}6.0x10^{10}$ BMC | 6 | ↓ Infarct size (% of dysfunctional segments) | LV angiography |
| Janssens et al. [21] | 33 vs. 34 controls | AMI / Randomized, Control + | Intracoronary | $4.8x10^8$ BMC | 4 | ↓ Infarct size (contrast-enhanced volume) | Contrast-enhanced MRI |
| ASTAMI [23] | 50 vs. 50 controls | AMI / Randomized, Sham - | Intracoronary | $6.8x10^7$ BMC | 6 | = Infarct size (contrast-enhanced volume/ number of scar segments) | Contrast-enhanced MRI Tc-99m tetrofosmin SPECT |
| TOPCARE-CHD [24] | 28 BMC vs.<br>24 CPC vs.<br>23 controls | CMI / Randomized, Sham - | Intracoronary | $2.1x10^8$ BMC<br>$2.2x10^7$ CPC | 3 | = Infarct size (contrast-enhanced volume) | Contrast-enhanced MRI |
| IACT [25] | 18 vs. 18 controls | CMI / Observational, Control + | Intracoronary | $9x10^7$ BMC | 3 | ↓ Infarct size (extent of dysfunctional area) | LV angiography |
| Katritsis et al. [26] | 11 vs. 11 controls | CMI / Observational, Control + | Intracoronary | $2\text{-}4x10^6$ BMC and EPC | 4 | ↓ Infarct size (number of scar segments) | Tc-99m sestamibi SPECT |
| Beeres et al. [29-31] | 25 | AP / Observational, Control - | Intramyocardial | $8.4x10^7$ BMC | 3 | = Infarct size (contrast-enhanced volume) | Contrast-enhanced MRI |
| Erbs et al. [34] | 13 vs. 13 controls | CTO / Randomized, Sham + | Intracoronary | $6.9x10^7$ G-CSF-mobilized cells | 3 | = Infarct size (contrast-enhanced volume) | Contrast-enhanced MRI |

AMI = acute myocardial infarction; AP = angina pectoris; BMC = bone marrow cells; CMI = chronic myocardial infarction; CPC = circulating progenitor cell; CTO = chronic total occlusion, EPC = endothelial progenitor cell; G-CSF = granulocyte-colony stimulating factor; LV = left ventricular; MRI = magnetic resonance imaging; Sham = placebo-controlled; SPECT = single photon emission computed tomography.

**Table 6** Effect of cell therapy on myocardial viability

| | No. of Patients | Setting / Study Design | Route of Delivery | Cell Type | Follow-up (months) | Main Findings | Technique Used |
|---|---|---|---|---|---|---|---|
| Strauer et al.[10] | 10 vs. 10 controls | AMI / Observational, Control + | Intracoronary | 2.8x$10^7$ BMC | 3 | = Contractile reserve | DSE |
| TOPCARE-AMI[11-14] | 29 BMC 30 CPC | AMI / Observational, Control - | Intracoronary | 2.1x$10^8$ BMC 1.6x$10^7$ CPC | 4 | ↑ F18-FDG uptake in infarct zone | F18-FDG PET |
| Fernández-Avilés et al.[18] | 20 vs. 13 controls | AMI / Observational, Control + | Intracoronary | 7.8x$10^7$ BMC | 6 | = Contractile reserve (dobutamine-induced ejection fraction) | DSE |
| Chen et al.[19] | 34 vs. 35 controls | AMI / Randomized, Sham + | Intracoronary | 4.8-6.0x$10^{10}$ BMC | 6 | ↑ F18-FDG uptake in infarct zone<br>↑ Linear local shortening<br>↑ Unipolar voltages | F18-FDG PET<br>Electromechanical mapping |
| Bartunek et al.[20] | 19 vs. 16 controls | AMI / Observational, Control + | Intracoronary | 1.3x$10^7$ BMC | 4 | ↑ F18-FDG uptake in infarct zone | F18-FDG PET |
| Janssens et al.[21] | 33 vs.34 controls | AMI / Randomized, Control + | Intracornary | 4.8x$10^8$ BMC | 4 | = Oxidative metabolism | C-11 acetate PET |
| IACT[25] | 18 vs. 18 controls | CMI / Observational, Control + | Intracoronary | 9x$10^7$ BMC | 3 | ↑ F18-FDG uptake in the infarct zone | F18-FDG PET |
| Katritsis et al.[26] | 11 vs. 11 controls | CMI / Observational, Control + | Intracoronary | 2-4x$10^6$ BMC and EPC | 4 | ↑ Number of viable segments | DSE |
| Beeres et al.[29-31] | 25 | AP / Observational, Control - | Intra-myocardial | 8.4x$10^7$ BMC | 3 | = Number of viable segments | F18-FDG SPECT |
| Perin et al.[32-33] | 14 vs. 7 controls | HF / Observational, Control + | Intra-myocardial | 3x$10^7$ BMC | 4 | ↑ lLnear local shortening<br>= Unipolar voltages | Electromechanical mapping |

AMI = acute myocardial infarction; AP = angina pectoris; BMC = bone marrow cells; CMI = chronic myocardial infarction; CPC = circulating progenitor cell; DSE = dobutamine stress echocardiography; EPC = endothelial progenitor cell; F18-FDG = F18-fluorodeoxyglucose; HF = heart failure; PET = positron emission tomography; Sham = placebo-controlled; SPECT = single photon emission computed tomography.

the scar tissue (i.e. nuclear imaging with PET or SPECT, contrast-enhanced MRI, myocardial contrast echocardiography), or indirect approaches that visualize the extent and severity of LV dysfunction (LV angiography, 2D echocardiography or cine MRI). Eight studies evaluated infarct size with SPECT or contrast-enhanced MRI, whereas 4 studies evaluated systolic dysfunction in the infarct zone as an indicator of extent of scar tissue. Seven of 12 studies demonstrated some reduction in infarct size, both in the setting of acute and chronic infarction.

The most accurate technique is contrast-enhanced MRI, allowing precise detection of scar tissue and currently the only technique discriminating between subendocardial and transmural infarction.[57] In the BOOST trial contrast-enhanced MRI was performed at baseline, at 6 and 18 months follow-up. At 18 months a mean reduction in infarct size of 13±12 ml was demonstrated in patients undergoing cell therapy, but control patients exhibited a comparable reduction in infarct size (10±13 ml; P=NS vs. patients undergoing cell therapy).[17] Of note, Ingkanisorn et al. recently demonstrated a significant reduction in infarct size on contrast-enhanced MRI performed at 1.7±0.8 days and 2 months following acute myocardial infarction.[58] Clearly, randomized controlled trials are needed to evaluate changes in infarct size after cell therapy as compared to the natural evolution after reperfused acute infarction.

**Myocardial Viability**

A total of 10 studies (in 243 patients) evaluated changes in viability after cell therapy (**Table 6**). Six studies were performed in the setting of acute infarction, 2 studies after chronic infarction, and 2 studies in patients with stress-induced ischemia. Follow-up ranged from 3 to 6 months after cell therapy.

The clinically available techniques for evaluation of viability include nuclear imaging with PET (mainly using F18-FDG, evaluating glucose utilization) or SPECT (with F18-FDG or Tc-99m-labeled agents), or low-dose dobutamine echocardiography (assessing contractile reserve). Contractile reserve can also be assessed by low-dose dobutamine MRI. Non-fluoroscopic catheter-based electromechanical mapping enables identification and localization of viable myocardial tissue by simultaneous assessment of electrical activation and local mechanical response.

Five studies used F18-FDG PET or SPECT to evaluate viability in the infarct zone of which 4 reported an increased F18-FDG uptake after cell therapy. For example, in the IACT study a mean increase of 15% in F18-FDG uptake in the infarct zone was demonstrated.[25] Similarly, in the TOPCARE-AMI study, mean F18-FDG uptake in the infarct zone increased from 55% to 58% at 4 months; however data on control patients were not available.[14]

Three studies used low-dose dobutamine echocardiography with 2 of 3 studies showing no improvement in contractile reserve, in contrast with the improvement observed in viability studies using F18-FDG PET. It should be noted that F18-FDG imaging reflects glucose utilization, whereas low-dose dobutamine echocardiography detects contractile

reserve. Although both parameters are markers of myocardial viability, not all viable myocardium may exhibit both contractile reserve and preserved glucose utilization. In patients with severely dysfunctional myocardium and extensive damage on the cellular level, contractile reserve is frequently lost, whereas glucose utilization is preserved.[59] Additional studies, evaluating different features of viable myocardium in the same patients are needed to elucidate changes in myocardial viability after cell therapy.

## Conclusions



The introduction of stem cell therapy for treatment of cell death-related heart diseases is promising but many issues remain unanswered, including mechanisms of benefit. Both pre-clinical and clinical studies have used non-invasive imaging techniques for in vivo tracking of stem cells and measurement of effect of therapy. For tracking, direct labeling of cells with radionuclides and super-paramagnetic agents has been reported; in addition, proof of concept of the use of reporter genes for cell tracking has been demonstrated. However, the majority of the methods available for cell tracking are currently only used in animal model studies.

In the clinical setting various imaging techniques including MRI, nuclear imaging with PET and SPECT, and echocardiography have been used to assess functional effects of cell therapy. Initial studies using these imaging techniques have mostly reported an improvement in LV function and myocardial perfusion/viability, with a reduction in infarct size. However, the evidence is limited and double-blind, randomized controlled trials with concurrent imaging techniques are needed to confirm and further elucidate beneficial effects of cell-based therapies. Moreover, future studies will need to assess the reproducibility and accuracy of the imaging methods used for cell tracking and evaluation of the functional effects. Finally, imaging on the molecular level is needed to better understand the effects of cell therapy. This will be realized with the use of PET-CT (or SPECT-CT) that permits co-registration of anatomical (CT) and functional (PET, SPECT) information and also with 3 (and higher) Tesla MRI.

# References


1. Wollert KC, Drexler H. Clinical applications of stem cells for the heart. Circ Res 2005;96:151-63.
2. Lev S, Kehat I, Gepstein L. Differentiation pathways in human embryonic stem cell-derived cardiomyocytes. Ann N Y Acad Sci 2005;1047:50-65.
3. Menasche P, Hagege AA, Scorsin M, et al. Myoblast transplantation for heart failure. Lancet 2001;357:279-80.
4. Smits PC, van Geuns RJ, Poldermans D, et al. Catheter-based intramyocardial injection of autologous skeletal myoblasts as a primary treatment of ischemic heart failure: clinical experience with six-month follow-up. J Am Coll Cardiol 2003;42:2063-9.
5. Kocher AA, Schuster MD, Szabolcs MJ, et al. Neovascularization of ischemic myocardium by human bone-marrow-derived angioblasts prevents cardiomyocyte apoptosis, reduces remodeling and improves cardiac function. Nat Med 2001;7:430-6.
6. Orlic D, Kajstura J, Chimenti S, et al. Bone marrow cells regenerate infarcted myocardium. Nature 2001;410:701-5.
7. Silva GV, Litovsky S, Assad JA, et al. Mesenchymal stem cells differentiate into an endothelial phenotype, enhance vascular density, and improve heart function in a canine chronic ischemia model. Circulation 2005;111:150-6.
8. Dawn B, Stein AB, Urbanek K, et al. Cardiac stem cells delivered intravascularly traverse the vessel barrier, regenerate infarcted myocardium, and improve cardiac function. Proc Natl Acad Sci U S A 2005;102:3766-71.
9. Messina E, De Angelis L, Frati G, et al. Isolation and expansion of adult cardiac stem cells from human and murine heart. Circ Res 2004;95:911-21.
10. Strauer BE, Brehm M, Zeus T, et al. Repair of infarcted myocardium by autologous intracoronary mononuclear bone marrow cell transplantation in humans. Circulation 2002;106:1913-8.
11. Assmus B, Schachinger V, Teupe C, et al. Transplantation of Progenitor Cells and Regeneration Enhancement in Acute Myocardial Infarction (TOPCARE-AMI). Circulation 2002;106:3009-17.
12. Britten MB, Abolmaali ND, Assmus B, et al. Infarct remodeling after intracoronary progenitor cell treatment in patients with acute myocardial infarction (TOPCARE-AMI): mechanistic insights from serial contrast-enhanced magnetic resonance imaging. Circulation 2003;108:2212-8.
13. Schachinger V, Assmus B, Britten MB, et al. Transplantation of progenitor cells and regeneration enhancement in acute myocardial infarction: final one-year results of the TOPCARE-AMI Trial. J Am Coll Cardiol 2004;44:1690-9.
14. Dobert N, Britten M, Assmus B, et al. Transplantation of progenitor cells after reperfused acute myocardial infarction: evaluation of perfusion and myocardial viability with FDG-PET and thallium SPECT. Eur J Nucl Med Mol Imaging 2004;31:1146-51.
15. Schachinger V, Assmus B, Honold, J et al. Normalization of coronary blood flow in the infarct-related artery after intracoronary progenitor cell therapy: intracoronary Doppler substudy of the TOPCARE-AMI trial. Clin Res Cardiol 2006;95:13-22.
16. Wollert KC, Meyer GP, Lotz J, et al. Intracoronary autologous bone-marrow cell transfer after myocardial infarction: the BOOST randomised controlled clinical trial. Lancet 2004;364:141-8.
17. Meyer GP, Wollert KC, Lotz J, et al. Intracoronary bone marrow cell transfer after myocardial infarction: eighteen months' follow-up data from the randomized, controlled BOOST (BOne marrOw transfer to enhance ST-elevation infarct regeneration) trial. Circulation 2006;113:1287-94.
18. Fernandez-Aviles F, San Roman JA, Garcia-Frade J, et al. Experimental and clinical regenerative capability of human bone marrow cells after myocardial infarction. Circ Res 2004;95:742-8.
19. Chen SL, Fang WW, Ye F, et al. Effect on left ventricular function of intracoronary transplantation of autologous bone marrow mesenchymal stem cell in patients with acute myocardial infarction. Am J Cardiol 2004;94:92-5.
20. Bartunek J, Vanderheyden M, Vandekerckhove B, et al. Intracoronary injection of CD133-positive enriched bone marrow progenitor cells promotes cardiac recovery after recent myocardial infarction: feasibility and safety. Circulation 2005;112:I178-I183.
21. Janssens S, Dubois C, Bogaert J, et al. Autologous bone marrow-derived stem-cell transfer in patients with ST-segment elevation myocardial infarction: double-blind, randomised controlled trial. Lancet 2006;367:113-21.

22. Schachinger V, Erbs S, Elsasser A, et al. Intracoronary bone marrow-derived progenitor cells in acute myocardial infarction. N Engl J Med 2006;355:1210-21.
23. Lunde K, Solheim S, Aakhus S, et al. Intracoronary injection of mononuclear bone marrow cells in acute myocardial infarction. N Engl J Med 2006;355:1199-209.
24. Assmus B, Honold J, Schachinger V, et al. Transcoronary transplantation of progenitor cells after myocardial infarction. N Engl J Med 2006;355:1222-32.
25. Strauer BE, Brehm M, Zeus T, et al. Regeneration of human infarcted heart muscle by intracoronary autologous bone marrow cell transplantation in chronic coronary artery disease: the IACT Study. J Am Coll Cardiol 2005;46:1651-8.
26. Katritsis DG, Sotiropoulou PA, Karvouni E, et al. Transcoronary transplantation of autologous mesenchymal stem cells and endothelial progenitors into infarcted human myocardium. Catheter Cardiovasc Interv 2005;65:321-9.
27. Fuchs S, Satler LF, Kornowski R, et al. Catheter-based autologous bone marrow myocardial injection in no-option patients with advanced coronary artery disease: a feasibility study. J Am Coll Cardiol 2003;41:1721-4.

28. Fuchs S, Kornowski R, Weisz G, et al. Safety and feasibility of transendocardial autologous bone marrow cell transplantation in patients with advanced heart disease. Am J Cardiol 2006;97:823-9.
29. Beeres SL, Bax JJ, Dibbets P, et al. Effect of intramyocardial injection of autologous bone marrow-derived mononuclear cells on perfusion, function, and viability in patients with drug-refractory chronic ischemia. J Nucl Med 2006;47:574-80.
30. Beeres SL, Bax JJ, Kaandorp TA, et al. Usefulness of intramyocardial injection of autologous bone marrow-derived mononuclear cells in patients with severe angina pectoris and stress-induced myocardial ischemia. Am J Cardiol 2006;97:1326-31.
31. Beeres SL, Bax JJ, Dibbets-Schneider P, et al. Sustained effect of autologous bone marrow mononuclear cell injection in patients with refractory angina pectoris and chronic myocardial ischemia: twelve-month follow-up results. Am Heart J 2006;152:684-6.
32. Perin EC, Dohmann HF, Borojevic R, et al. Transendocardial, autologous bone marrow cell transplantation for severe, chronic ischemic heart failure. Circulation 2003;107:2294-302.
33. Perin EC, Dohmann HF, Borojevic R, et al. Improved exercise capacity and ischemia 6 and 12 months after transendocardial injection of autologous bone marrow mononuclear cells for ischemic cardiomyopathy. Circulation 2004;110:II213-II218.
34. Erbs S, Linke A, Adams V, et al. Transplantation of blood-derived progenitor cells after recanalization of chronic coronary artery occlusion: first randomized and placebo-controlled study. Circ Res 2005;97:756-62.
35. Kang HJ, Kim HS, Zhang SY, et al. Effects of intracoronary infusion of peripheral blood stem-cells mobilised with granulocyte-colony stimulating factor on left ventricular systolic function and restenosis after coronary stenting in myocardial infarction: the MAGIC cell randomised clinical trial. Lancet 2004;363:751-6.
36. Frangioni JV, Hajjar RJ. In vivo tracking of stem cells for clinical trials in cardiovascular disease. Circulation 2004;110:3378-83.
37. Bellenger NG, Davies LC, Francis JM, et al. Reduction in sample size for studies of remodeling in heart failure by the use of cardiovascular magnetic resonance. J Cardiovasc Magn Reson 2000;2:271-8.
38. Hinds KA, Hill JM, Shapiro EM, et al. Highly efficient endosomal labeling of progenitor and stem cells with large magnetic particles allows magnetic resonance imaging of single cells. Blood 2003;102:867-72.
39. Hill JM, Dick AJ, Raman VK, et al. Serial cardiac magnetic resonance imaging of injected mesenchymal stem cells. Circulation 2003;108:1009-14.
40. Kraitchman DL, Heldman AW, Atalar E, et al. In vivo magnetic resonance imaging of mesenchymal stem cells in myocardial infarction. Circulation 2003;107:2290-3.
41. Kraitchman DL, Tatsumi M, Gilson WD, et al. Dynamic imaging of allogeneic mesenchymal stem cells trafficking to myocardial infarction. Circulation 2005;112:1451-61.
42. Shapiro EM, Skrtic S, Sharer K, et al. MRI detection of single particles for cellular imaging. Proc Natl Acad Sci U S A 2004;101:10901-6.
43. Lewin M, Carlesso N, Tung CH, et al. Tat peptide-derivatized magnetic nanoparticles allow in vivo tracking and recovery of progenitor cells. Nat Biotechnol 2000;18:410-4.
44. Bulte JW, Douglas T, Witwer B, et al. Magnetodendrimers allow endosomal magnetic labeling and in vivo tracking of stem cells. Nat Biotechnol 2001;19:1141-7.

45. Kostura L, Kraitchman DL, Mackay AM, et al. Feridex labeling of mesenchymal stem cells inhibits chondrogenesis but not adipogenesis or osteogenesis. NMR Biomed 2004;17:513-7.
46. Arbab AS, Yocum GT, Rad AM, et al. Labeling of cells with ferumoxides-protamine sulfate complexes does not inhibit function or differentiation capacity of hematopoietic or mesenchymal stem cells. NMR Biomed 2005;18:553-9.
47. Aicher A, Brenner W, Zuhayra M, et al. Assessment of the tissue distribution of transplanted human endothelial progenitor cells by radioactive labeling. Circulation 2003;107:2134-9.
48. Chin BB, Nakamoto Y, Bulte JW, et al. 111In oxine labelled mesenchymal stem cell SPECT after intravenous administration in myocardial infarction. Nucl Med Commun 2003;24:1149-54.
49. Barbash IM, Chouraqui P, Baron J, et al. Systemic delivery of bone marrow-derived mesenchymal stem cells to the infarcted myocardium: feasibility, cell migration, and body distribution. Circulation 2003;108:863-8.
50. Hofmann M, Wollert KC, Meyer GP, et al. Monitoring of bone marrow cell homing into the infarcted human myocardium. Circulation 2005;111:2198-202.
51. Penicka M, Widimsky P, Kobylka P, et al. Images in cardiovascular medicine. Early tissue distribution of bone marrow mononuclear cells after transcoronary transplantation in a patient with acute myocardial infarction. Circulation 2005;112:e63-e65.
52. Wu JC, Inubushi M, Sundaresan G, et al. Positron emission tomography imaging of cardiac reporter gene expression in living rats. Circulation 2002;106:180-3.
53. Krishnan M, Park JM, Cao F, et al. Effects of epigenetic modulation on reporter gene expression: implications for stem cell imaging. FASEB J 2006;20:106-8.
54. Wu JC, Chen IY, Sundaresan G, et al. Molecular imaging of cardiac cell transplantation in living animals using optical bioluminescence and positron emission tomography. Circulation 2003;108:1302-5.
55. Rodriguez-Porcel M, Gheysens O, Chen IY, et al. Image-guided cardiac cell delivery using high-resolution small-animal ultrasound. Mol Ther 2005;12:1142-7.
56. Cao F, Lin S, Xie X et al. In vivo visualization of embryonic stem cell survival, proliferation, and migration after cardiac delivery. Circulation 2006;113:1005-14.
57. Wagner A, Mahrholdt H, Holly TA, et al. Contrast-enhanced MRI and routine single photon emission computed tomography (SPECT) perfusion imaging for detection of subendocardial myocardial infarcts: an imaging study. Lancet 2003;361:374-9.
58. Ingkanisorn WP, Rhoads KL, Aletras AH, et al. Gadolinium delayed enhancement cardiovascular magnetic resonance correlates with clinical measures of myocardial infarction. J Am Coll Cardiol 2004;43:2253-9.
59. Sloof GW, Knapp FF Jr., van Lingen A, et al. Nuclear imaging is more sensitive for the detection of viable myocardium than dobutamine echocardiography. Nucl Med Commun 2003;24:375-81.